EQA - International Journal of Environmental Quality
ISSN 2281-4485 - Vol. 54 (2023):19-26
Journal homepage: https://eqa.unibo.it/

published by

Removal of Copper (II) and Lead (II) from hydrometallurgical effluent onto cellulose nanocomposites: mechanistic and Levenberg-Marquardt in Artificial Neural Network modelling

Musamba Banza*, Hilary Rutto

Clean Technology and Applied Materials Research Group, Department of Chemical and Metallurgical Engineering, Vaal University of Technology, South Africa.

- Corresponding Author Email: 208067310@edu.vut.ac.za

Article info
Received 6/2/2023; received in revised form 18/2/2023; accepted 19/2/2023
DOI: 10.6092/issn.2281-4485/16428

Abstract

A well-designed adsorption system should meet the requirements for high efficiency while remaining cost and time effective. nanocellulose materials have a proven track record as viable adsorbent alternatives. Cellulose is a renewable raw material that can be used to develop an adsorbent for heavy metal ions removal. In this study, CNCs were modified with EDTA and used as adsorbents to remove Pb(II) and Cu (II) ions from a mixture of metal ions synthesized solution. The modified CNCs were characterized using Fourier transform infrared (FTIR), X-ray diffraction (XRD), Scanning electron microscopy (SEM) and thermogravimetric analysis (TGA) surface area. SEM results showed that CNCs are porous, have narrow particles size, and FTIR results revealed that the functional group responsible for the lead ions removal was mainly carboxylates ($-COO^{2-}$). The XRD diffraction pattern showed that the CNCs possessed the cellulose crystalline configuration. The effects of the sorbent dosage, contact time, pH, and initial on the removal efficiency of the metal cations were examined. The absorption mechanism was described via four mechanistic models: Film diffusion, Weber and Morris, Dummwald-Wagner, and Bangham. The Artificial Neural Network (ANN) model predicted the adsorption of heavy metal ions with incredible accuracy, with an adsorption capacity of 250 mg/g for Copper and 270 mg/g for lead. Film diffusion was identified as the rate-limiting process via mechanistic modelling.

Keywords: *Cellulose nanocrystals, Nanocomposites, EDTA, Mechanistic, Artificial neural network.*

Introduction

Cellulose is the most common biopolymer found in nature. It has the chemical formula $(C_6H_{10}O_5)n$ and is a renewable, environmentally friendly, biodegradable, cheap, and non-toxic polymer (Shahnaz *et al.*, 2020). Each anhydroglucose unit includes three active hydroxyl groups: two secondary hydroxyl groups (C_2-OH, C_3-OH) and the leading hydroxyl group (C_6-OH)(Voisin *et al.*, 2017). These hydroxyl groups provide a high functionality to the cellulose molecule and its derivatives. It's widely employed in various sectors, including soft tissue replacement goods, construction materials, food packaging, and medication delivery(Hemmati *et al.*, 2018). Wood, straw, ramie fibres, bacterial cellulose, microcrystalline cellulose, and cotton are all examples of cellulose sources(Tang *et al.*, 2017). Additionally, cellulose is a semi-crystalline substance with both amorphous and crystalline areas. Acid is particularly prone to attacking and degrading amorphous areas because it is a structural flaw. Then, short monocrystalline nanoparticles known as CNCs are released(Du *et al.*, 2019). CNCs have a diameter of 1 to 100 nm, a length of 200 nm, and tangential dimen-

DOI: 10.6092/issn.2281-4485/16428

sions of 5 nm (Banza & Rutto, 2022a).

Furthermore, acid hydrolysis, enzymatic hydrolysis, oxidative degradation, and high-pressure homogenization can all be used to make CNCs(Danial *et al.*, 2015; Sun *et al.*, 2016). CNCs have recently attracted much attention because of their exciting properties compared to native cellulose, such as a large specific surface area, high crystallinity, availability, hydrophilicity, chirality, broad chemical modifying ability, biodegradability, biocompatibility, adequate strength and modulus, and unique optical properties. On the other hand, the CNC structure has many OH groups, resulting in significant reactivity and an excellent ability to interact with other groups(Liu & Kong, 2019). Similarly, CNC's large specific surface area and many actives OH groups make it easy to modify, resulting in excellent adsorption performance(Olad *et al.*, 2020). Esterification, etherification, oxidation, and polymer grafting are just a few of the chemical changes that CNC may do. These changes improve the uniform distribution of nanocrystals in aqueous solutions induced by electrostatic repulsion(Awang *et al.*, 2019; Ishak *et al.*, 2019).

Furthermore, enhancing the surface's negative charges makes it a suitable alternative for the adsorption of heavy metal ions and positively charged dyes with high adsorption capacity(Song *et al.*, 2019). Lead (II) and copper (II) are neurotoxic and non-biodegradable heavy metal ions commonly employed in metal polishing, electroplating, and paint applications(Wang *et al.*, 2017). Excessive exposure to lead and copper ions harms human health, primarily when found in our food. It can harm the endocrine, central nervous, cardiovascular, and brain cells(Hu *et al.*, 2018). Long-term use of water with high levels of lead ions can result in convulsions, renal failure, and cancer(Pawar *et al.*, 2016). Many methods have been used to remove Pb (II) and Cu (II), including ion exchange, biosorption, precipitation, adsorption, and reduction(Basu *et al.*, 2019; Kabuba & Banza, 2020; Vishnu Priyan *et al.*, 2021). Among these, the adsorption technique has been deemed more accessible and widely used to remove Pb (II) and Cu (II) pollution from aqueous solutions, owing to its numerous benefits, including high efficiency, cheap production costs, environmental friendliness, and ease of use(Borandegi & Nezamzadeh-Ejhieh, 2015; Onur *et al.*, 2019).

The Artificial Neural Network (ANN) is a computational model that estimates the processing data of biological neurons. In addition to input and output layers, most neural network models have one or more hidden layers; the type of investigation affects the number. A neural network's main characteristic is its capacity to perform internal computations to determine the targeted output from input information. Since ANN may be applied in complex systems since it is reliable and efficient in representing the non-linear interactions among the variables and responses of diverse processes, by training the multiple input-output networks algorithm, the ANN can also assess multifactorial non-linear and complicated processes given sufficient data(Ayoola *et al.*, 2019)

Furthermore, four mechanistic models (Weber and Morris, Dummwald-Wagner Film diffusion, and Bangham models) were investigated to determine the rate-controlling phase in the adsorption process. To evaluate the models, the coefficient of correlation was utilized. As a consequence, the objectives of this study are as follows: (1) Cellulose nanocrystals (CNCs) modified adsorbent production and characterization; (2) utilizing ANN to predict the adsorption capacity of Cu (II) and Pb (II); and (3) using four mechanistic models to determine the rate-controlling phase of the adsorption process.

Materials and methods

Materials

Cellulose nanocrystals (CNCs) were extracted from millet husk waste from a millet farm in Kenya; sodium hydroxide(98%), nitric acid (70%), ethylenediaminetetraacetic acid (EDTA) (99%), lead nitrate (99%), and hydrochloric acid (36%) are all analytical grade and were purchased from Sigma Aldrich.

Modification of CNCs

0.01 M ethylenediaminetetraacetic acid (EDTA) was added to the reactor containing 25 g of CNCs for 120 minutes at a speed of 150 rpm. The agitation duration was increased to 8 hours after introducing 50 mL of hydrochloric acid 0.1 M. The changed product was centrifuged at 1500 rpm for 15 minutes and washed with distilled water to remove unreacted chemicals until the pH reached 7.

Characterization of CNCs

Fourier transform infrared spectroscopy investigated

DOI: 10.6092/issn.2281-4485/16428

the functional groups found in CNCs and the resulting structural changes (FTIR, Varian 7000). SEM was used to examine the morphological surface of the CNCs (SEM, Philips XL30FEG). The qualitative and quantitative evaluations were completed using X-ray diffraction (XRD, Philips expert 0993). The thermal stability of the CNCs was determined using a thermal thermogravimetric analyzer (TGA, NETZSCH5 209F3).

Adsorption experiments

Batch experiments in the thermostatic shaker were conducted in a 500 mL beaker. Pb (II) from the wastewater solution was removed for 5 hours at 150 rpm using modified CNCs with EDTA. 5 g of modified CNCs were mixed with a conical flask containing 250 mL of the heavy metal ion solution. The initial concentration was 50 to 500 mg/L, the pH was 2 to 8, and the temperature was 25 to 40 degrees Celsius. 25 mL of the mixture's suspension was filtered every one-hour interval, and the resulting solutions were examined using ICP (Induced Coupled Plasma, Icap7000).

The following equation was used to determine the adsorption capacities at any time t (qt, $mg.g^{-1}$):

$$q_t = \frac{(C_{i-}C_t)\times V}{Ma} \qquad [1]$$

where Ci (mg/L) represents the initial Pb (II) and Cu (II) concentration, Ct (mg/L) represents the concentration at time t, Ma (mg) represents the mass of dry CNCs used, and V (L) represents the volume of Pb (II) solution used for selective removal.

Table 1 shows the range of variables used for the ANN.

Input	Range	Output
1. pH	3-9	Adsorption capacity (mg/g)
2. Concentration Ni (II)	50-500	
3. Time (min)	0-120	
4. dosage blend hydrogel (mg/L)	5-20	
5. Temperature (K)	298-318	

Table 1
The range of variables used for the models

Results and discussion

FTIR analysis

As shown in Figure1, the distinct absorption peaks about 3300, 2800, and 1750 cm^{-1}, confirming the stretching shaking of O-H and the asymmetric and symmetric vibrations of C-C of the COOH group, respectively(Danial *et al.*, 2015). Furthermore, the bands at 1500 cm^{-1} are connected to the CH_2 expansion and contraction. The strong band at 1040 cm-1 is ascribed to the pyranose C-O-C skeletal vibration, whereas the weak band at 890 cm-1 is assigned to the overall cellulose structure with glucoside connections. For modified CNCs, the peaks of the -OH of -COOH signal are stronger and broader, causing the signal to be harsher. CNCs may have been successfully changed due to this (Banza & Rutto, 2022b). These results demonstrate that the hydroxyl and carboxyl groups on the modified CNCs surface were significant in the selective removal process.

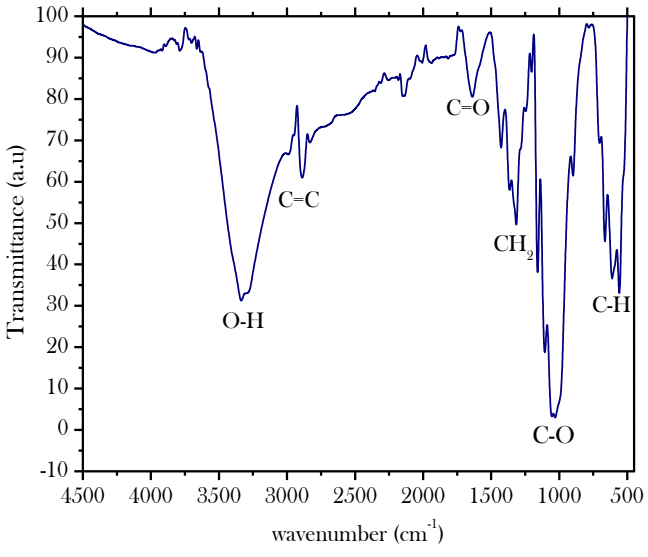

Figure 1. *FTIR spectra of CNCs nanocomposites*

SEM analysis

CNCs have a networked rod-like structure, as seen in Figure 2, with some tangled and wrinkled edges and a compact network structure (Olad *et al.*, 2020). These morphological alterations on the CNCs surface might be caused by the ethylenediaminetetraacetic acid modification, extensive hydrogen bonding between nanocrystals, and chemical bonds produced

DOI: 10.6092/issn.2281-4485/16428

during the modification process.

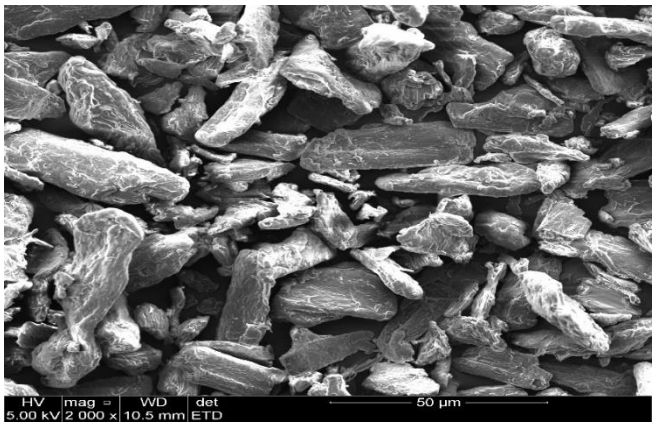

Figure 2. *SEM image of CNCs nanocomposites*

X-Ray diffraction (XRD)

As shown in Figure 3, the crystallinity of CNCs was investigated using an X-ray diffractometer. Furthermore, the CNCs characteristic peaks of 18.0, 25.3, and 40.0 are comparable with cellulose type I (Kargarzadeh *et al.*, 2015). According to the findings, the modification of CNCs with ethylenediamine-tetraacetic acid has little influence on the crystallinity of the CNCs generated.

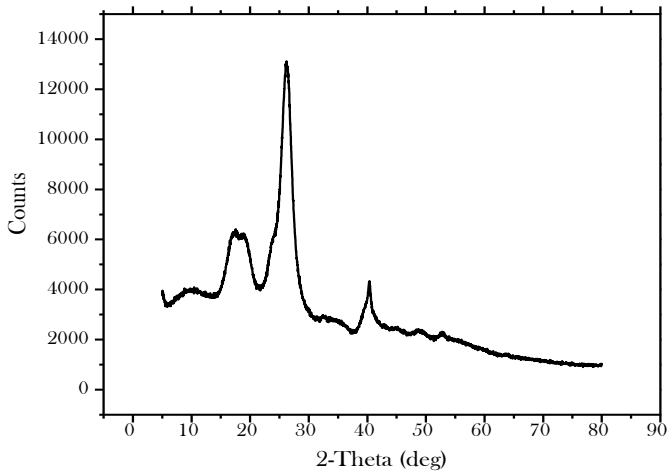

Figure 3. *XRD spectra of CNCs nanocomposite*

Thermal stability analysis

TGA curves of CNCs samples collected in an N_2 atmosphere at a 10 °C min^{-1} heating rate are shown in Figure 4. The evaporation of remaining H_2O and moisture from the samples causes the first degradation process (0-100°C), which results in weight losses of 15 %. The thermal disintegration of the CNCs polymer caused the second degradation process to occur at higher temperatures (200-450°C). A third degradation stage occurred at 450–600°C, resulting in an additional 10% weight loss, demonstrating the effective modification process (Hu *et al.*, 2018).

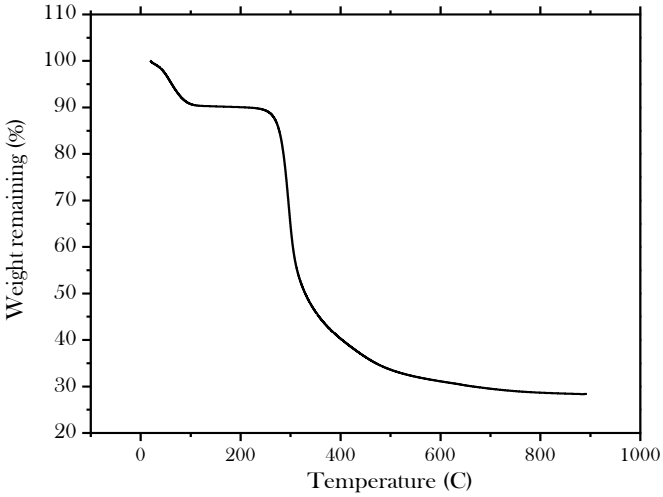

Figure 4 *TGA curves of the studied CNCs*

Adsorption studies

Figures 5(a, b) show the results of batch tests. The pH solution significantly impacted Pb (II) and Cu (II) removal from modified CNCs, with the maximum adsorption capacity of 270 mg/g and 250 mg/g for Pb (II) and Cu (II) reported at pH 6. Because of proton ion competition with metallic cations in a very acidic media and the influence of hydroxyl anions on metallic cation precipitation at high pH. The removal effectiveness was reduced at lower pH values due to an increase (protons) in positive charge density on the surface sites, which causes repulsion between metal ions and groups with a positive charge on the surface (Hemmati *et al.*, 2018). The adsorption capacity reduced from 265 mg/g to 245 mg/g when the temperature climbed from 298 to 318 °C for Pb (II) and from 245 mg/g to 220 mg/g when the temperature climbed from 298 to 318 °C for Cu (II), as shown in Figure 5 (c) and (d). The temperature of the solution/solid interface and the process's kinetic properties are significant variables in this process. Because of the mobility and competitiveness of Pb (II) and Cu (II) ions on modified CNCs at higher temperatures, the adsorption capacity will decrease as the temperature rises. A temperature rise creates an increase in energy, which causes molecules to collide, lowering

DOI: 10.6092/issn.2281-4485/16428

the likelihood of Pb (II) and Cu (II) being bound to the accessible active sites (Kabuba & Banza, 2020b).

Modeling of artificial neural network

To assess adsorption efficiency, all calculations were performed with Origin 2019b, and the modular artificial neural networks were constructed with a NN toolbox using MATLAB 2017a mathematical software. In Figure 6, a three-layer system is set up with a four-neuron input layer (starting concentration, solution pH, contact time, temperature, and adsorbent dose), a hidden layer with nine different modes, and a single neuron on the output layer (5-15-2). The most common network is Back-Propagation (BP-ANN), which employs a first-order gradient descent technique to train an algorithm for modelling experimental data. It's a good algorithm for decreasing mistakes with each iteration. Among the several Back-Propagation (BP) strategies, we choose for the Marquardt-Levenberg (LM) learning strategy. For Pb (II) and Cu (II) adsorption simulation and prediction, the log-sigmoid transfer function (log sig) in the hidden layer with four neurons in the first layer and a linear transfer function in the output node were used for all data sets in ANN (David *et al.*, 2021).

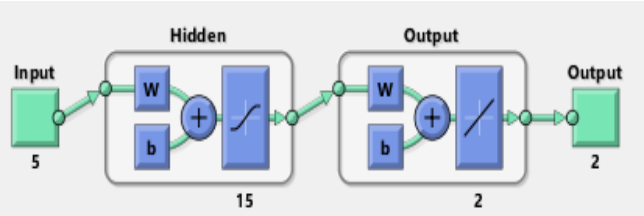

Figure 6. *The architecture of ANN model*

Figure 7 depicts the network's interaction with the training, testing, and validation data. The correlation coefficients for training, testing, and validation datawere calculated to be 0.990, 0.994, 0.999, and

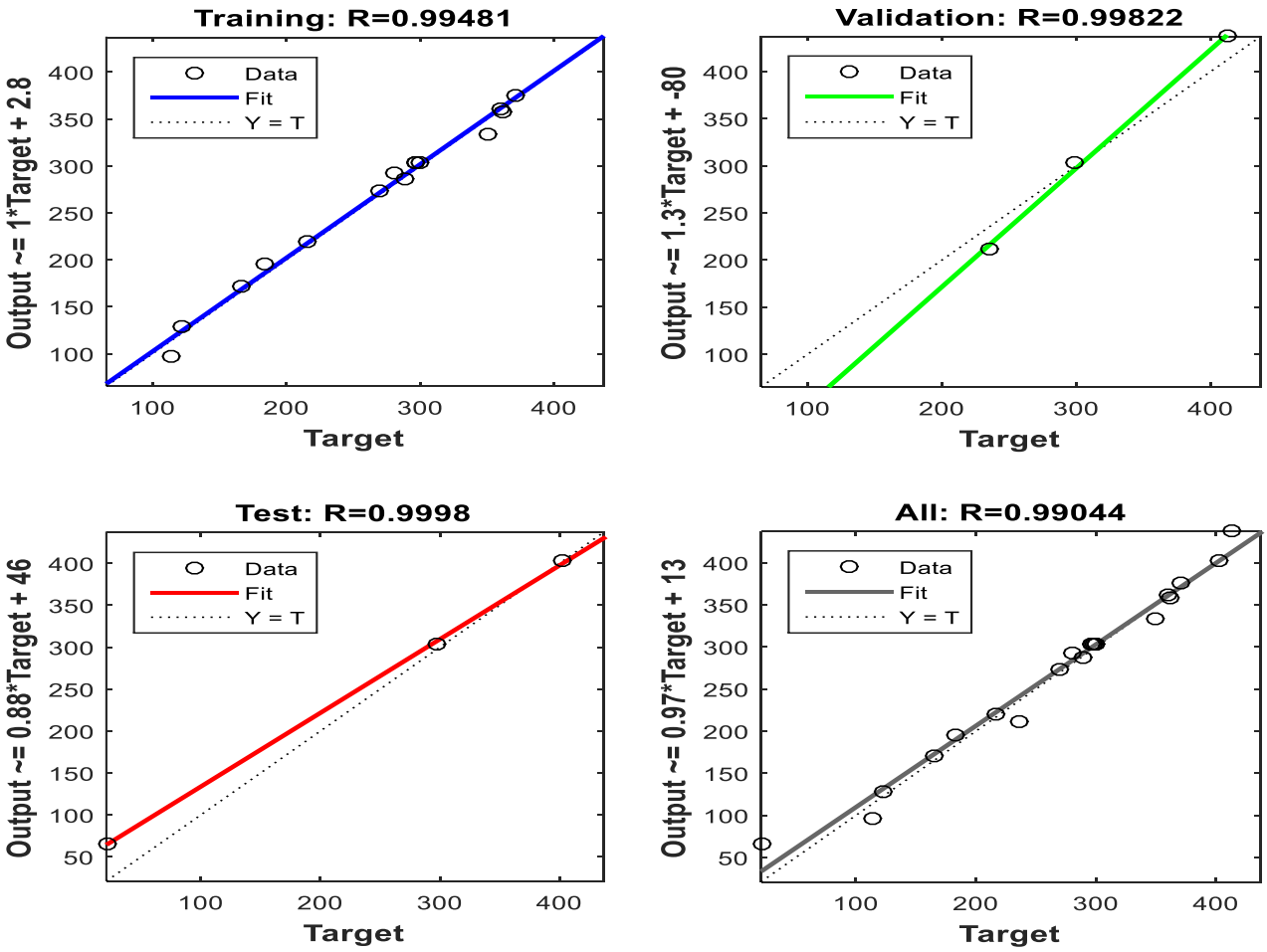

Figure 7. *The architecture of artificial neural network*

DOI: 10.6092/issn.2281-4485/16428

0.998, respectively. In addition, the straight line depicts the linear connection.The model's projected (output) data and experimental (target) data are correlated. The findings suggest that the actual and model-predicted data are in good agreement. Consequently, the overall correlation coefficient (0.990) illustrates the developed ANN model's exceptional prediction capacity.

The best method for training, testing, and validation was Levenberg-Marquardt, as illustrated in Figure 8. As seen by the decreased Means Square Errors (MSE), this shows that the network's predicted output is equal to the laboratory analyses' findings. This method offered the best structure since it had the lowest MSE value. This suggests that the Levenberg-Marquardt approach is appropriate for training the ANN Toolbox to estimate the Pb (II) and Cu (II) adsorption.

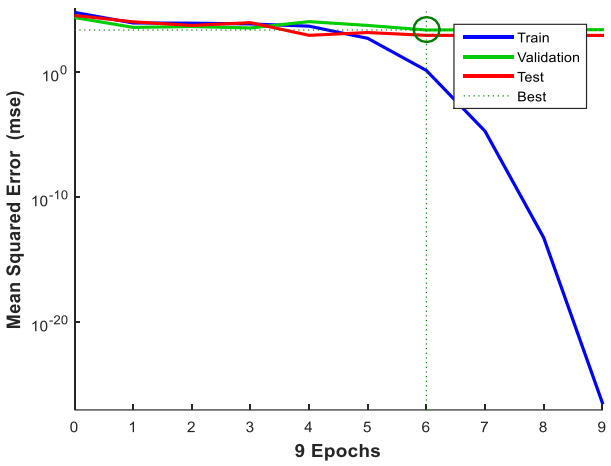

Figure 8. *Performance of the Levenberg-Marquardt algorithm*

Mechanistic modelling

The model constants are summarized in Table 2. The correlation coefficient for the intra-particle diffusion model is 0.934 and 0.925 for Pb (II) and Cu (II). The removal of Pb (II) and Cu (II) was not limited merely by intra-particle diffusion since C is not equal to 0. The Dumwald-Wagner model was investigated using a plotting of $\log(1-A^2)$ as a function of time t. The Dumwald-Wagner model is an intra-particle model. The high fit of the near-linear fit indicated that pore dispersion was implicated in the removal mechanism. The Bangham method was assessed using the log (Ca/Ca−qmax) as a factor of log t. The model was used to analyse if pore dispersion was the only rate-limiting step in the adsorption mechanism. The liquid film diffusion model was evaluated by showing ln(1- A) vs time. The gradient of the linear plot was used to calculate the rate factor. The R^2 of 0.988 for Pb (II) and 0.985 for Cu (II) suggests that the adsorption is controlled by film diffusion, with time and proportional approach to optimum being linearly connected. The rate constant Kd decreased as the solute uptake time increased (Kabuba and Banza, 2021)

Model	parameter	Pb (II)	Cu(II)
Liquid film diffusion	K_d (min^{-1})	0.081	0.073
	R^2	0.988	0.985
Weber and Morris	K_X ($mg/g.min^{0.5}$)	0.351	0.254
	C_X (mg/g)	13.20	11.98
	R^2	0.934	0.925
Dumwald-Wagner	K_{DW}	0.062	0.057
	R^2	0.912	0.891
Bangham	K_b	0.581	0.458
	β	0.195	0.157
	R^2	0.944	0.932

Table 2. *Mechanistic model parameters for Pb (II) and Cu (II) removal*

Reusability study

Indeed, from an economical perspective, it is critical to explore the potential of adsorbent materials to be regenerated and reused. Using an appropriate desorption solution, we may utilise the adsorbent repeatedly for the adsorption of heavy metal ions. es.

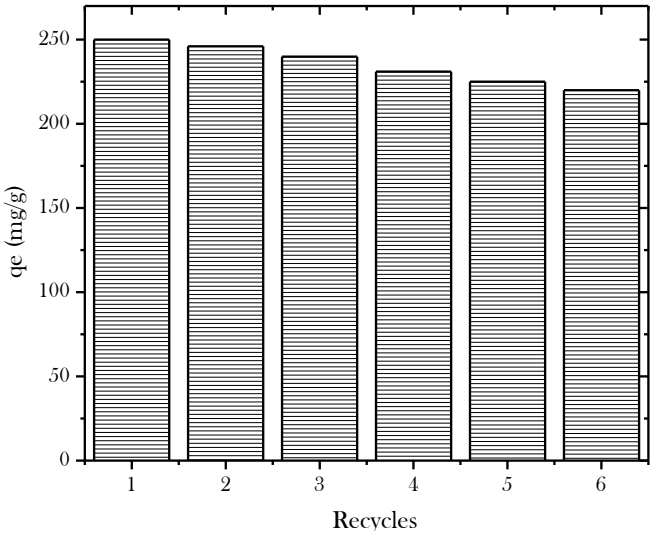

Figure 6 *Reusability cycles of CNCs nanocomposites.*

DOI: 10.6092/issn.2281-4485/16428

Our experiment used HCl solution as a regeneration and desorption agent for CNCs. A dominating protonation reaction occurs between the hydrogen ions in the solution and the existing COO– groups on the CNCs surface. As a result, the ionic interaction between Pb(II) and Cu(II) ions and COO– is destroyed, and CNCs renewal occurs. Figure 6 demonstrates that the adsorption capacity of CNCs dropped marginally as the number of cycles increased up to 6 times.

Conclusion

In this study, EDTA and cellulose nanocrystals were used to develop the nanocomposites to remove Pb (II) and Cu (II), and the viability of ANN prediction abilities was examined. The existence of OH and COOH indicates that cellulose nanocrystals were effectively used to generate the nanocomposites. The effectiveness of the synthesis process by FTIR, SEM, XRD and TGA analysis was confirmed by the uniformity in the breakdown of cellulose nanocrystals and EDTA. The interaction effects of process factors and their optimum conditions were determined. The ideal conditions were determined to be an initial pH of 6, a temperature of 298 K, and an adsorption capacity of 250 mg/g for Cu (II) and 270 mg/g for Pb (II). ANN approaches with the BP algorithm are described and compared to experimental data. The Levenberg Marquardts Algorithm (5-15-2) with a tangent sigmoid transfer function at the hidden layer and a linear transfer function at the output layer produced the minimum MSE. According to mechanistic modelling, the most likely rate-controlling phase of the removal process was film diffusion

Acknowledgements

The author would like to thank the Vaal University of Technology's Department of Chemical & Metallurgical Engineering for providing operating facilities

Data statement

The data supporting this study's findings are available on request from the corresponding author. The data are not publicly available due to privacy or ethical restrictions.

Declaration of Competing Interest

The authors declare that they have no known competing for financial interests or personal relationships that could have influenced the work reported in this paper.

References

AWANG N.W., RAMASAMY D., KADIRGAMA K., SAMYKANO M., NAJAFI G., AZWADI N., SIDIK C. (2019) International Journal of Heat and Mass Transfer An experimental study on characterization and properties of nano lubricant containing Cellulose Nanocrystal (CNC). International Journal of Heat and Mass Transfer, 130:1163–1169. https://doi.org/10.1016/j.ijheatmass transfer. 2018.11.041

AYOOLA A.A., HYMORE F.K., OMONHINMIN C.A., OLAWOLE O.C., FAYOMI O.S.I., BABA-TUNDE D., FAGBIELE O. (2019) Analysis of waste groundnut oil biodiesel production using response surface methodology and artificial neural network. Chemical Data Collection, 22:100238. https://doi.org/10.1016/j.cdc. 2019.100238

BANZA M., RUTTO H. (2022A). Toxic / Hazardous Substances and Environmental Engineering Continuous fixed-bed column study and adsorption modeling removal of Ni , Cu , Zn and Cd ions from synthetic acid mine drainage by nanocomposite cellulose hydrogel. Journal of Environental Science and Health Part A, 57 (2), 117-129. https://doi.org/10.1080/10934529.2022.2036552

BANZA M., RUTTO H. (2022B) Extraction of cellulose nanocrystals from millet (Eleusine coracana) husk waste: optimization using Box Behnken design in response surface methodology (RSM). International Nano Letter, 12(3):257–272. https://doi.org/10.1007/s40089-022-00369-x

BASU, H., SAHA, S., MAHADEVAN, I.A., & PIMPLE, M.V. (2019). Journal of Water Process Engineering Humic acid coated cellulose derived from rice husk : A novel biosorbent for the removal of Ni and Cr. Journal Water Process Engineering. 32:100892. https://doi.org/10.1016/j.jwpe.2019.100892

BORANDEGI, M. & NEZAMZADEH-EJHIEH, A. (2015). Enhanced removal efficiency of clinoptilolite nano-particles toward Co(II) from aqueous solution by modification with glutamic acid. Colloids Surfaces A Physicochemical. Engineering Aspect, 479:35–45. http://dx.doi.org/10.1016/j.colsurfa.2015.03.040

DANIAL W.H., ABDUL MAJID Z., MOHD MUHID M.N., TRIWAHYONO S., BAKAR M.B., RAMLI Z. (2015) The reuse of wastepaper for the extraction of cellulose nanocrystals. *Carbohydrate Polymer*s, 118:165–169. http://dx.doi.org/10.1016/j.carbpol.2014.10.072

DAVID S., ADEKOJO O., WAHEED M., TAHERI-GARAVAND A., VERMA T.N., DAIRO O.U., BOLAJI B.O., AFZAL A. (2021) Prandtl number of optimum biodiesel from food industrial waste oil and diesel fuel blend for diesel engine. *Fuel*, 285:119049. https://doi.org/

DOI: 10.6092/issn.2281-4485/16428

10.1016/j.fuel.2020.119049

DU H., LIU W., ZHANG M., SI C., ZHANG X., LI B. (2019) Cellulose nanocrystals and cellulose nano fi brils based hydrogels for biomedical applications. Carbohydrate Polymers, 209:130–144. https://doi.org/10.1016/j.carbpol.2019.01.020

HEMMATI F., MAHDI S., KASHANINEJAD M., BARANI M. (2018) International Journal of Biological Macromolecules Synthesis and characterization of cellulose nanocrystals derived from walnut shell agricultural residues. International Journal of Biological Macromolecules, 120:1216–1224. https://doi.org/10.1016/j.ijbiomac.2018.09.012

HU Z., MOHAMED A., YU D. (2018) International Journal of Biological Macromolecules Fabrication of carboxylated cellulose nanocrystal / sodium alginate hydrogel beads for adsorption of Pb (II) from aqueous solution, 108:149–157. https://doi.org/10.1016/j.carbpol.2019.01.020

ISHAK N.S., ISHAK K.M.K., BUSTAMI Y., ROKIAH H. (2019) Evaluation of Cellulose Nanocrystals (CNCs) as Protein Adsorbent in stick water. Material. Today Procedia, 17:516–524. https://doi.org/10.1016/j.matpr.2019.06.330

KABUBA J., BANZA M. (2020) Results in Engineering Ion-exchange process for the removal of Ni (II) and Co (II) from wastewater using modi fi ed clinoptilolite : Modeling by response surface methodology and arti fi cial neural network. Results Engineering, 8:100189. https://doi.org/10.1016/j.rineng.2020.100189

KABUBA J., BANZA M. (2021). Modification of clinoptilolite with dialkylphosphinic acid for the selective removal of cobalt (II) and nickel (II) from hydrometallurgical effluent. The Canadian Journal of Chemical Engineering, 99: S168-S178. https://doi.org/10.1002/cjce.24005

KARGARZADEH, H., SHELTAMI, R.M., AHMAD, I., ABDULLAH, I., & DUFRESNE, A. (2015). Cellulose nanocrystal : A promising toughening agent for unsaturated polyester nanocomposite. Polymers, 56:346–357. http://dx.doi.org/10.1016/j.polymer.2014.11.054

LIU, L. & KONG, F. (2019). In vitro investigation of the influence of nano-cellulose on starch and milk digestion and mineral adsorption. International Journal of Biological and Macromolecules, 137:1278–1285. https://doi.org/10.1016/j.ijbiomac.2019.06.194

OLAD A., DOUSTDAR F., GHAREKHANI H. (2020) Fabrication and characterization of a starch-based superabsorbent hydrogel composite reinforced with cellulose nanocrystals from potato peel waste. Colloids Surfaces a Physicochemical Engineering Aspect, 601: 124962. https://doi.org/10.1016/j.colsurfa.2020.124962

ONUR A., SHANMUGAM K., NG A., GARNIER G., BATCHELOR W. (2019) Cellulose fibre- perlite depth filters with cellulose nanofibre top coating for improved filtration performance. Colloids Surfaces Aspect, 583: 123997. https://doi.org/10.1016/j.colsurfa.2019.123997

PAWAR, R.R., LALHMUNSIAMA, BAJAJ, H.C., & LEE, S.M. (2016). Activated bentonite as a low-cost adsorbent for the removal of Cu(II) and Pb(II) from aqueous solutions: Batch and column studies. Journal of Industrial Engineering Chemistry, 34:213–223. http://dx.doi.org/10.1016/j.jiec.2015.11.014

SHAHNAZ, T., S., M.M.F., V.C., P., & NARAYANASAMY, S. (2020). Surface modification of nanocellulose using polypyrrole for the adsorptive removal of Congo red dye and chromium in binary mixture. International Journal of Biological Macromolecules, 151:322–332. https://doi.org/10.1016/j.ijbiomac. 2020.02.181

SONG, K., QIAN, X., LI, X., ZHAO, Y., & YU, Z. (2019). Fabrication of a novel functional CNC cross-linked and reinforced adsorbent from feather biomass for e ffi cient metal removal. Carbohydrydrate Polymers, 222: 115016. https://doi.org/10.1016/j.carbpol.2019.115016

SUN, B., YU, H.Y., ZHOU, Y., HUANG, Z., & YAO, J.M. (2016). Single-step extraction of functionalized cellulose nanocrystal and polyvinyl chloride from industrial wallpaper wastes. Industrial Crops Production, 89: 66–77. http://dx.doi.org/10.1016/j.indcrop.2016.04.040

TANG, J., SISLER, J., GRISHKEWICH, N., & TAM, K.C. 2017. Journal of Colloid and Interface Science Functionalization of cellulose nanocrystals for advanced applications. Journal of Colloid Interface Science, 494: 397–409. http://dx.doi.org/10.1016/j.jcis.2017.01.077

VISHNU PRIYAN, V., SHAHNAZ, T., SUGANYA, E., SIVAPRAKASAM, S., & NARAYANASAMY, S. (2021). Ecotoxicological assessment of micropollutant Diclofenac biosorption on magnetic sawdust: phyto, microbial and fish toxicity studies. Journal of Hazardous Materials. 403: 123532. https://doi.org/10.1016/j.jhazmat.2020.123532

VOISIN H., BERGSTRÖ, L., LIU P., MATHEW A.P. (2017) Nanocellulose-Based Materials for Water Purification. Nanomaterials, 7(3):57. https://doi.org/10.3390/ nano7030057

WANG N., JIN R., OMER A.M., OUYANG X. (2017) International Journal of Biological Macromolecules Adsorption of Pb (II) from fish sauce using carboxylated cellulose nanocrystal : isotherm, kinetics, and thermodynamic studies. International Journal of Biological Macromolecules, 102:232–240. http://dx.doi.org/10.1016/j.ijbiomac.2017.03.150